

# Nonlinearity compensation using dispersion-folded digital backward propagation

Likai Zhu<sup>1,\*</sup> and Guifang Li<sup>1,2</sup>

<sup>1</sup>CREOL, The College of Optics and Photonics, University of Central Florida, 4000 Central Florida Boulevard, Orlando, Florida 32816, USA

<sup>2</sup>li@creol.ucf.edu

\*likaizhu@creol.ucf.edu

**Abstract:** A computationally efficient dispersion-folded (D-folded) digital backward propagation (DBP) method for nonlinearity compensation of dispersion-managed fiber links is proposed. At the optimum power level of long-haul fiber transmission, the optical waveform evolution along the fiber is dominated by the chromatic dispersion. The optical waveform and, consequently, the nonlinear behavior of the optical signal repeat at locations of identical accumulated dispersion. Hence the DBP steps can be folded according to the accumulated dispersion. Experimental results show that for 6,084 km single channel transmission, the D-folded DBP method reduces the computation by a factor of 43 with negligible penalty in performance. Simulation of inter-channel nonlinearity compensation for 13,000 km wavelength-division multiplexing (WDM) transmission shows that the D-folded DBP method can reduce the computation by a factor of 37.

©2012 Optical Society of America

**OCIS codes:** (060.2330) Fiber optics communications; (060.1660) Coherent communications; (190.4370) Nonlinear optics, fibers.

---

## References and links

1. G. P. Agrawal, *Nonlinear Fiber Optics* (Academic Press, Elsevier, 2001).
2. P. P. Mitra and J. B. Stark, "Nonlinear limits to the information capacity of optical fibre communications," *Nature* **411**(6841), 1027–1030 (2001).
3. B. C. Kurtzke, "Suppression of fiber nonlinearities by appropriate dispersion management," *IEEE Photon. Technol. Lett.* **5**(10), 1250–1253 (1993).
4. K. Mukasa, K. Imamura, I. Shimotakahara, T. Yagi, and K. Kokura, "Dispersion compensating fiber used as a transmission fiber: inverse/reverse dispersion fiber," *J. Opt. Fiber Commun. Rep.* **3**(5), 292–339 (2006).
5. E. Ip, A. P. T. Lau, D. J. F. Barros, and J. M. Kahn, "Coherent detection in optical fiber systems," *Opt. Express* **16**(2), 753–791 (2008).
6. S. J. Savory, G. Gavioli, R. I. Killely, and P. Bayvel, "Electronic compensation of chromatic dispersion using a digital coherent receiver," *Opt. Express* **15**(5), 2120–2126 (2007).
7. H. Sun, K.-T. Wu, and K. Roberts, "Real-time measurements of a 40 Gb/s coherent system," *Opt. Express* **16**(2), 873–879 (2008).
8. E. Yamazaki, S. Yamanaka, Y. Kisaka, T. Nakagawa, K. Murata, E. Yoshida, T. Sakano, M. Tomizawa, Y. Miyamoto, S. Matsuoaka, J. Matsui, A. Shibayama, J. Abe, Y. Nakamura, H. Noguchi, K. Fukuchi, H. Onaka, K. Fukumitsu, K. Komaki, O. Takeuchi, Y. Sakamoto, H. Nakashima, T. Mizuochi, K. Kubo, Y. Miyata, H. Nishimoto, S. Hirano, and K. Onohara, "Fast optical channel recovery in field demonstration of 100-Gbit/s Ethernet over OTN using real-time DSP," *Opt. Express* **19**(14), 13179–13184 (2011).
9. J. M. Kahn and K.-P. Ho, "A bottleneck for optical fibres," *Nature* **411**(6841), 1007–1010 (2001).
10. E. B. Desurvire, "Capacity demand and technology challenges for lightwave systems in the next two decades," *J. Lightwave Technol.* **24**(12), 4697–4710 (2006).
11. A. D. Ellis, J. Zhao, and D. Cotter, "Approaching the non-linear Shannon limit," *J. Lightwave Technol.* **28**(4), 423–433 (2010).
12. R.-J. Essiambre, G. Kramer, P. J. Winzer, G. J. Foschini, and B. Goebel, "Capacity limits of optical fiber networks," *J. Lightwave Technol.* **28**(4), 662–701 (2010).
13. L. Li, Z. Tao, L. Liu, W. Yan, S. Oda, T. Hoshida, and J. C. Rasmussen, "XPM tolerant adaptive carrier phase recovery for coherent receiver based on phase noise statistics monitoring," in *Proc. ECOC'09*, Paper P3.16 (2009).
14. K.-P. Ho and J. M. Kahn, "Electronic compensation technique to mitigate nonlinear phase noise," *J. Lightwave Technol.* **22**(3), 779–783 (2004).
15. L. B. Du and A. J. Lowery, "Practical XPM compensation method for coherent optical OFDM systems," *IEEE Photon. Technol. Lett.* **22**(5), 320–322 (2010).

16. K. Roberts, C. Li, L. Strawczynski, M. O'Sullivan, and I. Hardcastle, "Electronic precompensation of optical nonlinearity," *IEEE Photon. Technol. Lett.* **18**(2), 403–405 (2006).
17. X. Li, X. Chen, G. Goldfarb, E. F. Mateo, I. Kim, F. Yaman, and G. Li, "Electronic post-compensation of WDM transmission impairments using coherent detection and digital signal processing," *Opt. Express* **16**(2), 880–888 (2008).
18. E. Ip and J. M. Kahn, "Fiber impairment compensation using coherent detection and digital signal processing," *J. Lightwave Technol.* **28**(4), 502–519 (2010).
19. D. S. Millar, S. Makovejs, C. Behrens, S. Hellerbrand, R. I. Killey, P. Bayvel, and S. J. Savory, "Mitigation of fiber nonlinearity using a digital coherent receiver," *IEEE J. Sel. Top. Quantum Electron.* **16**(5), 1217–1226 (2010).
20. O. V. Sinkin, R. Holzlohner, J. Zweck, and C. R. Menyuk, "Optimization of the split-step Fourier method in modeling optical-fiber communications systems," *J. Lightwave Technol.* **21**(1), 61–68 (2003).
21. S. Oda, T. Tanimura, T. Hoshida, C. Ohshima, H. Nakashima, Z. Tao, and J. C. Rasmussen, "112 Gb/s DP-QPSK transmission using a novel nonlinear compensator in digital coherent receiver," in *Proc. OFC'09, Paper OThR6* (2009).
22. E. F. Mateo, L. Zhu, and G. Li, "Impact of XPM and FWM on the digital implementation of impairment compensation for WDM transmission using backward propagation," *Opt. Express* **16**(20), 16124–16137 (2008).
23. E. F. Mateo, F. Yaman, and G. Li, "Efficient compensation of inter-channel nonlinear effects via digital backward propagation in WDM optical transmission," *Opt. Express* **18**(14), 15144–15154 (2010).
24. Q. Zhang and M. I. Hayee, "Symmetrized split-step Fourier scheme to control global simulation accuracy in fiber-optic communication systems," *J. Lightwave Technol.* **26**(2), 302–316 (2008).
25. L. B. Du and A. J. Lowery, "Improved single channel backpropagation for intra-channel fiber nonlinearity compensation in long-haul optical communication systems," *Opt. Express* **18**(16), 17075–17088 (2010).
26. D. Rafique, M. Mussolin, M. Forzati, J. Mårtensson, M. N. Chugtai, and A. D. Ellis, "Compensation of intra-channel nonlinear fibre impairments using simplified digital back-propagation algorithm," *Opt. Express* **19**(10), 9453–9460 (2011).
27. L. Zhu and G. Li, "Folded digital backward propagation for dispersion-managed fiber-optic transmission," *Opt. Express* **19**(7), 5953–5959 (2011).
28. L. Zhu, X. Li, E. F. Mateo, and G. Li, "Complementary FIR filter pair for distributed impairment compensation of WDM fiber transmission," *IEEE Photon. Technol. Lett.* **21**(5), 292–294 (2009).
29. J. K. Fischer, C.-A. Bunge, and K. Petermann, "Equivalent single-span model for dispersion-managed fiber-optic transmission systems," *J. Lightwave Technol.* **27**(16), 3425–3432 (2009).
30. C. Xie, "WDM coherent PDM-QPSK systems with and without inline optical dispersion compensation," *Opt. Express* **17**(6), 4815–4823 (2009).
31. V. Curri, P. Poggiolini, A. Carena, and F. Forghieri, "Dispersion compensation and mitigation of nonlinear effects in 111-Gb/s WDM coherent PM-QPSK systems," *IEEE Photon. Technol. Lett.* **20**(17), 1473–1475 (2008).
32. T. Yoshida, T. Sugihara, H. Goto, T. Tokura, K. Ishida, and T. Mizuochi, "A study on statistical equalization of intra-channel fiber nonlinearity for digital coherent optical systems," in *Proc. ECOC'11, Tu.3.A.* (2011).
33. J. P. Gordon and L. F. Mollenauer, "Phase noise in photonic communications systems using linear amplifiers," *Opt. Lett.* **15**(23), 1351–1353 (1990).
34. T. Tanimura, T. Hoshida, T. Tanaka, L. Li, S. Oda, H. Nakashima, Z. Tao, and J. C. Rasmussen, "Semi-blind nonlinear equalization in coherent multi-span transmission system with inhomogeneous span parameters," in *Proc. OFC'10, OMR6* (2010).
35. L. Zhu, F. Yaman, and G. Li, "Experimental demonstration of XPM compensation for WDM fibre transmission," *Electron. Lett.* **46**(16), 1140–1141 (2010).

---

## 1. Introduction

Optical signal is distorted by noise, dispersion and nonlinearity in fiber transmission. The Kerr nonlinearity, an intensity dependence of the refractive index, induces impairments including self-phase modulation (SPM), cross-phase modulation (XPM) and four-wave mixing (FWM) [1]. These nonlinear impairments increase with the optical signal power. As a tradeoff between high signal to noise ratio and low nonlinear impairment, there is an optimum power level for a fiber transmission system, corresponding to a maximal spectral efficiency [2].

In most of the installed fiber links, chromatic dispersion is compensated by cascading fibers with inverse dispersion parameters [3]. With the advent of new dispersion compensating fibers (DCF), wide-band dispersion flatness has been obtained by compensating for both dispersion and dispersion slope [4]. In the emerging digital coherent transmission systems [5], electronic dispersion compensation (EDC) can be realized using digital signal processing (DSP) [6–8]. As the compensation technique of linear distortions matured, fiber nonlinearity has become the limiting factor to further increase the capacity and distance of the next generation fiber-optic transmission systems [9–12].

In [13], an adaptive filtering carrier phase recovery method was proposed to suppress the nonlinear phase noise due to XPM. Lumped phase de-rotation proportional to the received single-channel or multi-channel optical intensity can also be used for SPM compensation [14] or XPM compensation [15], respectively. However, the lump phase de-rotation method is based on the assumption that the intensity waveform remains unchanged throughout the fiber propagation. In long-haul broadband transmission where the chromatic dispersion causes significant pulse reshaping and inter-channel walk-off, a distributed nonlinearity compensation method, known as digital backward propagation (DBP), is necessary for the effective compensation of the joint effect of dispersion and nonlinearity [16–19]. In order for DBP to be accurate, a small step size is usually required, resulting in a large number of steps and a heavy computational load [20].

Some methods have been proposed to reduce the computational load of DBP [20–28]. In comparison with inter-channel nonlinearity compensation, intra-channel nonlinearity compensation usually requires a smaller number of steps because the step size is not limited by the inter-channel walk-off effect [20,21]. In comparison with solving the nonlinear Schrodinger equation (NLSE) for the total field of the WDM signal, solving the coupled NLSE was suggested for inter-channel nonlinearity compensation because it requires a smaller step number and a lower sampling rate [22]. The step number can be further reduced by factorizing the dispersive walk-off effects in the DBP algorithm [23] and using variable step size [20,24,25]. We recently proposed a distanced-folded DBP method for dispersion-managed links with complete dispersion compensation in every fiber span [27,29]. However, most of the deployed fiber links has non-zero residual dispersion per span in order to avoid the resonant nonlinear effects [30,31]. In [32], an efficient scheme based on statistical approximation of accumulated nonlinear phase rotation with discrete residual dispersion was demonstrated for intra-channel nonlinearity compensation. In this paper, we propose and demonstrate a computationally efficient dispersion-folded (D-folded) DBP method that is effective for fiber links with arbitrary dispersion maps.

## 2. Dispersion-folded DBP method

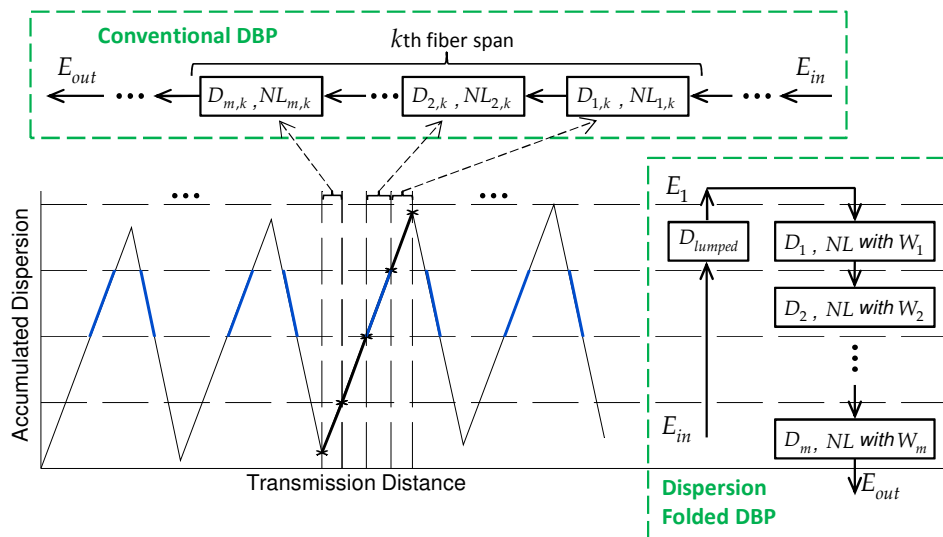


Fig. 1. Conventional DBP and D-folded DBP for a dispersion-managed coherent fiber link.

The dispersion map of a typical dispersion-managed fiber transmission system is illustrated in Fig. 1. After the dispersion-managed fiber transmission and coherent detection, conventional DBP can be performed in the backward direction of the fiber propagation. Multiple steps are required for each of the many fiber spans, resulting in a large number of steps.

At the optimum power level of fiber transmission, the total nonlinear phase shift is on the order of 1 radian [33]. Therefore, in long-haul transmission, the nonlinear effect in each fiber span is weak, and the optical waveform evolution along the fiber is dominated by the chromatic dispersion. Under the weakly nonlinear assumption, the optical waveform repeats at locations where accumulated dispersions are identical. Since the Kerr nonlinear effects are determined by the instantaneous optical field, the nonlinear behavior of the optical signal also repeats at locations of identical accumulated dispersion. Hence we can fold the DBP according to the accumulated dispersion.

The propagation of the optical field,  $E(z, t)$ , is governed by

$$\frac{\partial E(z, t)}{\partial z} = [D + \varepsilon \cdot N(|E(z, t)|^2)] \cdot E(z, t), \quad (1)$$

where  $D$  is the linear operator for dispersion, fiber loss and amplifier gain,  $N(|E(z, t)|^2)$  is the nonlinear operator,  $\varepsilon$  (to be set to unity) is a parameter indicating that the nonlinear perturbation is small for the reasons given above.

The solution of Eq. (1) can be written as,

$$E(z, t) = E_l(z, t) + \varepsilon \cdot E_{nl}(z, t). \quad (2)$$

Substituting Eq. (2) into Eq. (1), expanding the equation in power series of  $\varepsilon$ , and equating to zero the successive terms of the series, we have

$$\frac{\partial E_l(z, t)}{\partial z} = D \cdot E_l(z, t), \quad (3)$$

$$\frac{\partial E_{nl}(z, t)}{\partial z} = D \cdot E_{nl}(z, t) + N(|E_l(z, t)|^2) \cdot E_l(z, t), \quad (4)$$

which describe the linear evolution and the nonlinear correction, respectively. It is noted that the nonlinear correction  $E_{nl}(z, t)$  is governed by a linear partial differential equation with nonzero forcing which depends on the linear solution only.

It is shown in Fig. 1 that the dispersion map can be divided into  $m$  divisions as indicated by the horizontal dashed lines. The fiber segments within a division have the same accumulated dispersion. Based on the principle of superposition, the total nonlinear correction is the sum of nonlinear corrections due to nonzero forcing at each fiber segment.

In conventional DBP, the contribution from each fiber segment is computed separately. However, it is advantageous to calculate the total nonlinear correction as the sum of nonlinear corrections due to nonzero forcing at different accumulated dispersion divisions, each having multiple fiber segments. This is because, with the exception of different input power levels and effective lengths, the linear component  $E_l(z, t)$  that generates the nonlinear correction and the total dispersion for the generated nonlinear perturbation to reach the end of the transmission are identical for the fiber segments with the same accumulated dispersion. Therefore, the nonlinear corrections due to these multiple fiber segments with the same accumulated dispersion are identical except a constant and can be calculated all at once using a weighting factor as described below.

In D-folded DBP, the fiber segments with the same accumulated dispersion (e.g., the blue solid lines) can be folded into one step. For a fiber link with positive residual dispersion per span, a lumped dispersion compensator ( $D_{lumped}$ ) can be used to obtain the optical field ( $E_l$ ) in the first dispersion division. Then dispersion compensation ( $D$ ) and nonlinearity compensation ( $NL$ ) are performed for each of the subsequent dispersion divisions. To take into account the different power levels and effective lengths of the fiber segments, a

weighting factor ( $W_i$ ) is used in the nonlinearity compensator of each step. The nonlinear phase shift in the  $i$  th step of D-folded DBP is given by  $\varphi_i = W_i \cdot |\bar{E}_i(t)|^2$ , where  $\bar{E}_i(t)$  is the optical field with the power normalized to unity. The weighting factor is given by  $W_i = \sum_k \gamma \int P_{i,k}(z) dz$ , where  $P_{i,k}(z)$  is the power level as a function of distance within the  $k$  th fiber segment in the  $i$  th dispersion division. The effect of loss for each fiber segment is taken into account in the calculation of this weighting factor.

The D-folded DBP theory derived above is based on the NLSE for fiber propagation thus can be applied to not only intra-channel [32] but also inter-channel nonlinearities as we show below. In comparison to [32], the D-folded DBP also takes into account the effect of dispersion on the perturbative nonlinear effects. The commonality in [27], [32], and the D-folded DBP presented here is that nonlinearity compensation for multiple fiber segments is performed in a single step, resulting in orders of magnitude savings in computation. Using the split-step method for D-folded DBP, the linear and nonlinear effects can be de-coupled when the step size is small enough. The dispersion within a fiber segment is neglected in a nonlinearity compensation operator. Meanwhile, the power level, effective length and nonlinear coefficient of a fiber segment have been taken into account in the calculation of the nonlinear phase shift. Thus the DBP can be folded even if the fiber link consists of multiple types of fibers. Note that calculating the weighting factors does not require real-time computation.

### 3. Experimental results

To demonstrate the effectiveness of the D-folded DBP, we performed the experiment of single-channel 6,084 km transmission of NRZ-QPSK signal at 10 Gbaud. The experimental setup is shown in Fig. 2(a). At the transmitter, carrier from an external-cavity laser is modulated by a QPSK modulator using a  $2^{23}-1$  pseudo random bit sequence (PRBS). The single-polarization optical signal is launched into a recirculating loop controlled by two acousto-optic modulators (AOMs). The recirculating loop consists of two types of fibers: 82.6 km standard single mode fiber (SSMF) with 0.2 dB/km loss and  $83 \mu\text{m}^2$  effective area, and 11 km DCF with 0.46 dB/km loss and  $20 \mu\text{m}^2$  effective area. By optimizing the performance in the training experiments of EDC, the dispersion of the SSMF and the DCF are determined as 17.06 ps/nm/km and  $-123.35$  ps/nm/km, respectively. The residual dispersion per span (RDPS) is 53 ps/nm. Two erbium doped fiber amplifiers (EDFAs) are used to completely compensate for the loss in the loop. An optical bandpass filter (BPF) is used to suppress the EDFA noise. At the receiver, the signal is mixed with the local oscillator from another external cavity laser in a  $90^\circ$  hybrid after the polarizations are aligned with a polarization controller (PC). The I and Q components of the received signal are detected using two photo-detectors (PDs). A real-time oscilloscope is used for analog-to-digital conversion and data acquisition at 40 Gsamples/s. The DSP is performed off-line with Matlab. Note that for realistic terrestrial systems, the parameters of the fiber spans may not be available with good accuracy. Attempts are being made at estimating the link parameters for conventional DBP [34]. Estimation of link parameters for D-folded DBP needs further investigation.

Without loss of generality, we solve the NLSE using the asymmetric Split-Step Fourier Method (SSMF) with one dispersion compensator per step [24]. For long-haul transmission, the DBP step size is usually limited by dispersion [20]. In this paper, we use DBP steps with equal dispersion per step for simplicity. The Q-value as a function of the number of steps is shown in Fig. 2(b). The required number of steps to approach the maximum Q-value can be reduced from 1,300 to 30 by using the D-folded DBP. The number of multiplications per sample (MPS) for DBP is reduced by a factor of 43 (see details in the Appendix). There is a trade-off between complexity and performance using either conventional DBP or D-folded DBP. A Q-value of 10.2 dB, corresponding to a 1.1 dB improvement in comparison with EDC, can be achieved using 130-step conventional DBP or 5-step D-folded DBP.

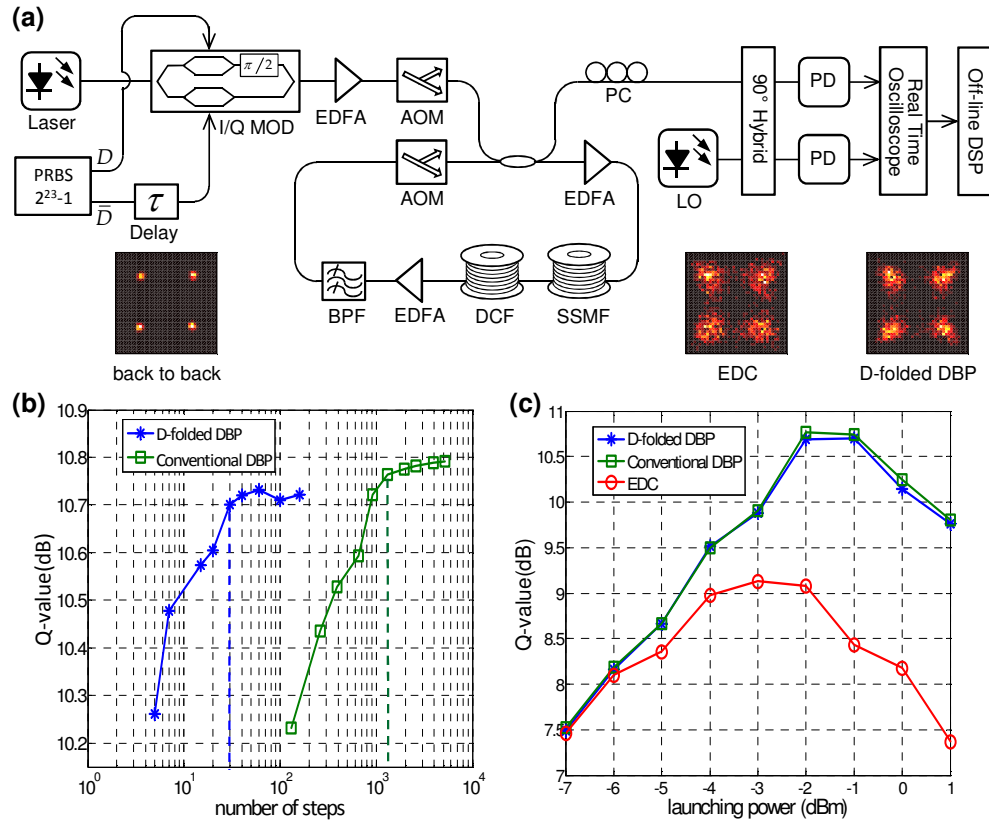


Fig. 2. Experimental demonstration of D-folded DBP. (a) Experimental setup. Inset: constellations after back-to-back detection, EDC and DBP at the corresponding optimum power levels. (b) Q-value as a function of the number of steps using conventional DBP (green line) and D-folded DBP (blue line). (c) Q-value as a function of optical launching power after EDC (red line), 30-step D-folded DBP (blue line) and 1,300-step conventional DBP (green line).

Figure 2(c) shows the Q-value as a function of the launching power. With only EDC for the accumulated residual dispersion, the maximum Q-value is 9.1 dB. With nonlinearity compensation using D-folded DBP, the maximum Q-value is increased to 10.7 dB. The performance after the 30-step D-folded DBP is almost the same as that after the 1,300-step conventional DBP. The Q-values and computational load are shown in Table 1.

**Table 1. Performance and complexity of conventional DBP and D-folded DBP for the single channel system**

method	Q-value (dB)	number of steps	MPS
conventional	10.7	1,300	13,385
D-folded	10.7	30	314

#### 4. Simulation results

We performed the simulation of wavelength-division multiplexing (WDM) transmission as illustrated in Fig. 3(a) using the VPITransmissionMaker. At the transmitter, 12 channels of 56 Gb/s NRZ-QPSK signal are transmitted with 50 GHz channel spacing. The QPSK modulators are driven by  $2^{23}-1$  PRBS sequences. Each PRBS generator is assigned with a unique random bit seed for de-correlation. The linewidth of the lasers is 100 kHz. The dispersion managed fiber link consists of 260 spans of the OFS UltraWave SLA/IDF Ocean Fiber combination. In each 50 km span, the SLA fiber with a large effective area is used near the EDFA, followed

by the IDF fiber with inverse dispersion and dispersion slope. The loss, dispersion, relative dispersion slope and effective area of the SLA fiber are 0.188 dB/km, 19.5 ps/nm/km, 0.003/nm and  $106 \mu\text{m}^2$ , respectively. The corresponding parameters for the IDF fiber are 0.23 dB/km,  $-44 \text{ ps/nm/km}$ , 0.003/nm and  $31 \mu\text{m}^2$ , respectively. The RDPS is determined by the proportion of SLA fiber to IDF fiber in each span. The noise figure of the EDFAs is 4.5 dB. After de-multiplexing and coherent detection, 8192 symbols from each channel are saved at a sampling rate of 56 Gsamples/s. Then the DSP is performed with Matlab.

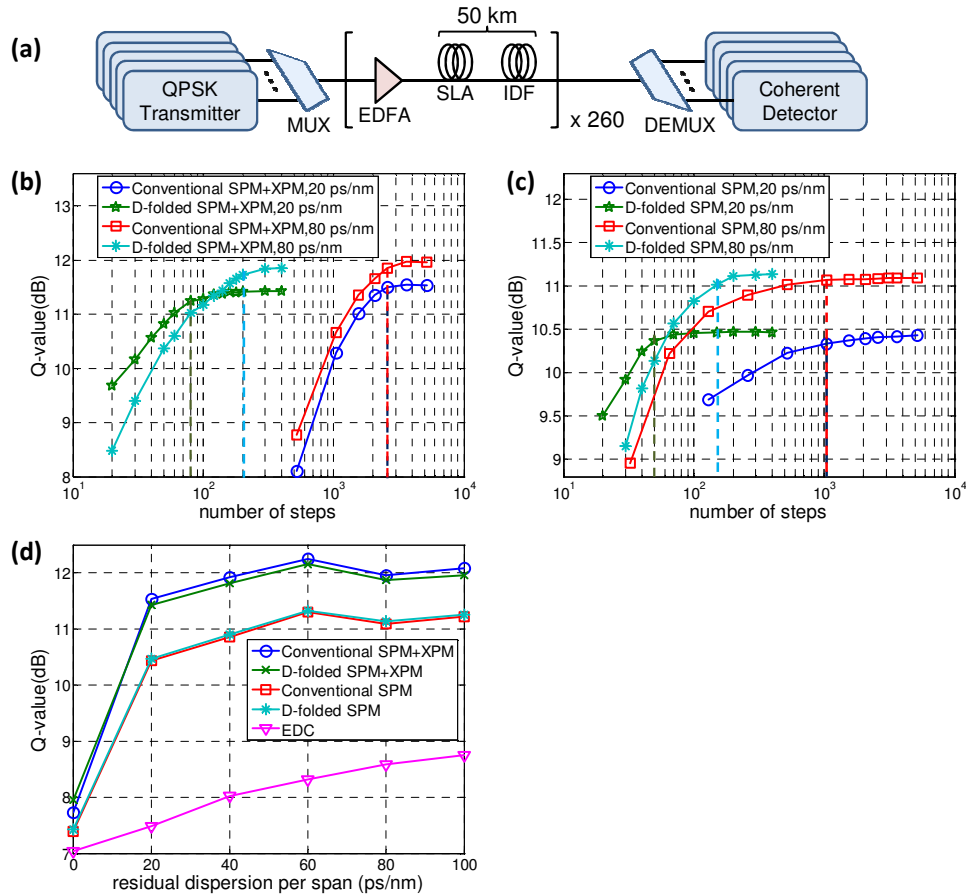


Fig. 3. Numerical demonstration of D-folded DBP for WDM transmission. (a) Block diagram of the dispersion-managed WDM system. (b) Q-value as a function of the number of steps using D-folded DBP and conventional DBP for SPM + XPM compensation. (c) Q-value as a function of the number of steps using D-folded DBP and conventional DBP for SPM compensation. (d) Q-value as a function of residual dispersion per span.

In DBP for SPM + XPM compensation, coupled NLSE is solved with the asymmetric SSFM [35]. The inter-channel walk-off effects are considered in the nonlinearity compensation operators in order to increase the required step size [23]. For each channel, the XPM from two neighboring channels and the SPM are compensated. Simulation results show that the XPM from the other channels is weak because of the walk-off effect.

The average Q-value of all the WDM channels is calculated after 13,000 km transmission and DSP. The Q-values are calculated through variance estimation on the constellations under the assumption of Gaussian distribution. The Q-values presented here only provide a metric for comparison between different compensation schemes and are not reliable for the computation of bit error ratios because correlations exist in the nonlinear noise even after nonlinearity compensation. Figure 3(b) shows the Q-value as a function of the number of

steps after DBP for SPM + XPM compensation using conventional DBP and D-folded DBP. With a RDPS of 20 ps/nm, the Q-values after 2,600-step conventional DBP and 80-step D-folded DBP are 11.5 dB and 11.3 dB, respectively. The minimum multiplications per sample for the 2,600-step conventional DBP and the 80-step D-folded DBP are 51,422 and 1,393, respectively. The computational load is reduced by a factor of 37 with a penalty of 0.2 dB in Q-value. With a RDPS of 80 ps/nm, the Q-values after 2,600-step conventional DBP and 200-step D-folded DBP are 11.9 dB and 11.7 dB, respectively. The step sizes of conventional DBP and D-folded DBP are usually limited by chromatic dispersion. As a result, with a larger RDPS, a larger number of steps for D-folded DBP are required to approach the maximum Q-value. Note that in realistic systems, exchanging information between channels for XPM compensation can increase the complexity of the DSP implementation.

Figure 3(c) shows the Q-value as a function of the number of steps after the DBP for SPM compensation. With a RDPS of 20 ps/nm, the Q-values after 1,040-step conventional DBP and 50-step D-folded DBP are 10.3 dB and 10.4 dB, respectively. The number of multiplications per sample is reduced from 10,400 to 408 with no penalty in Q-value. With a RDPS of 80 ps/nm, the Q-values after 1,040-step conventional DBP and 150-step D-folded DBP are 11.1 dB and 11.0 dB, respectively. The Q-values and computational loads are summarized in Table 2.

**Table 2. Performance and complexity of conventional DBP and D-folded DBP for the WDM system**

RDPS (ps/nm)	method	Q-value (dB)	number of steps	MPS
20	conventional (SPM + XPM)	11.5	2,600	51,422
	D-folded (SPM + XPM)	11.3	80	1,393
	conventional (SPM)	10.3	1,040	12,222
	D-folded (SPM)	10.4	50	500
80	conventional (SPM + XPM)	11.9	2,600	51,422
	D-folded (SPM + XPM)	11.7	200	3,829
	conventional (SPM)	11.1	1,040	12,222
	D-folded (SPM)	11.0	150	1,544

Recently, coherent systems with EDC for dispersion-unmanaged fiber links have been implemented. The minimum multiplications per sample for EDC of a 13,000 km dispersion-unmanaged fiber link using SLA fiber is 245.

The Q-value obtained after DBP with sufficiently large number of steps as a function of the RDPS is shown in Fig. 3(d). For the dispersion-managed link, as the RDPS increases, the Q-value after EDC increases because the nonlinear effects and the span loss decrease. With DBP, the Q-value approaches the maximum value when the RDPS is larger than 20 ps/nm. In comparison with EDC, the DBP with XPM compensation can increase the Q-value by more than 3 dB when the RDPS is larger than 20 ps/nm. The performance using D-folded DBP is almost the same as that using conventional DBP.

## 5. Conclusion

In conclusion, we have proposed a dispersion-folded DBP method that can significantly reduce the computational load of DBP for fiber nonlinearity compensation. Experimental results show that the computation of DBP for 6,084 km single channel transmission can be reduced by a factor of 43. Simulation of a WDM system shows that the D-folded DBP method can reduce the computation for XPM compensation by a factor of 39.

## Appendix: calculation of the computational load

The computational load can be associated to the number of complex multiplications per sample (MPS) involved in the operation. Either time-domain [using finite-impulse response (FIR) filters] or frequency-domain equalization can be used for the compensation of dispersion. In DBP, the frequency response of each dispersion compensator must be very accurate in order to minimize the error accumulation. When the amount of dispersion to be compensated and thus the theoretical minimum number of taps of the FIR filter are small, the

number of taps required for the FIR filter can be much larger than the minimum number corresponding to the group delay [28]. Therefore, frequency-domain overlap-add FFT method is assumed here for calculating the computational complexity of DBP in this paper [20].

For an overhead length  $P$ , a signal block length  $M$  is chosen to minimize the computational load using the radix-2 Fast Fourier Transform (FFT) with an FFT block size of  $(M + P)$ . For EDC, the overhead is approximately given by  $P = 2\pi|\beta_2|B \cdot h \cdot S$  where  $\beta_2$ ,  $B$ ,  $h$  and  $S$  are the dispersion, signal bandwidth per channel, fiber length and sampling rate, respectively. The MPS for the overlap-add filtering is given by  $[(M + P)\log_2(M + P) + (M + P)]/M$ . For the EDC of the 13,000 km dispersion-unmanaged link, we consider an FFT block size of  $2^{10}$  which is practical for the current electronic technology. By using 11 overlap-add filtering operators with  $M = 548$  and  $P = 476$ , the minimum possible MPS is 245.

To ensure accuracy of the dispersion operator in DBP, we assume an overhead  $P$  that is 3 times the group delay  $2\pi|\beta_2|B \cdot h \cdot S$ . In the nonlinearity operator of DBP, the calculations of the optical intensity and the nonlinear phase shift each costs one complex multiplication. The value of the nonlinear phase shift can be obtained using a lookup table. The MPS of DBP for SPM compensation is given by  $n_{st} \cdot [(M + P)\log_2(M + P) + (M + P) + 2M]/M$ , where  $n_{st}$  is the step number. For the 6,084 km single channel transmission, the minimum MPSs of the 1,300-step conventional DBP and the 30-step D-folded DBP are 13,385 and 314, respectively. For the SPM compensation of the 13,000 km WDM system, the minimum MPSs of the 1,040-step conventional DBP and the 50-step D-folded DBP are 12,222 and 500, respectively.

In the DBP with XPM compensation for the 13,000 km WDM transmission, the length of the inter-channel walk-off filter is given by  $P = 2\pi|\beta_2|\Delta f \cdot h \cdot S$  where  $\Delta f$  is the channel spacing. The MPS for DBP is given by  $n_{st} \cdot [2(M + P)\log_2(M + P) + 3(M + P) + 2M]/M$ . The minimum MPS for the 2,600-step conventional DBP is 51,422. For the 80-step D-folded DBP, the minimum MPS is 1,393.